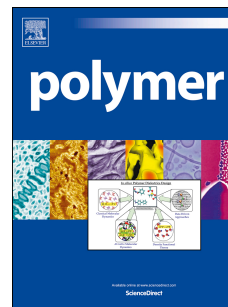


# Accepted Manuscript

Columnar Liquid Crystalline Polyglycidol derivatives: A novel alternative for proton-conducting membranes

Xavier Montané, Suryakant Vilasrao Bhosale, José Antonio Reina, Marta Giamberini



PII: S0032-3861(15)00317-1

DOI: [10.1016/j.polymer.2015.03.071](https://doi.org/10.1016/j.polymer.2015.03.071)

Reference: JPOL 17743

To appear in: *Polymer*

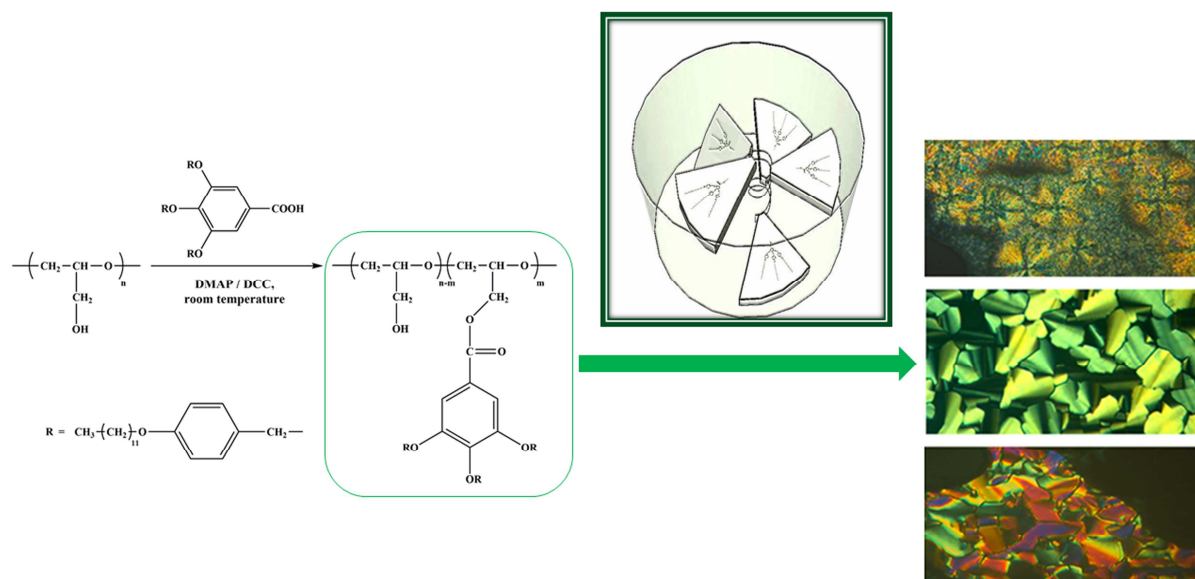
Received Date: 28 January 2015

Revised Date: 25 March 2015

Accepted Date: 26 March 2015

Please cite this article as: Montané X, Bhosale SV, Reina JA, Giamberini M, Columnar Liquid Crystalline Polyglycidol derivatives: A novel alternative for proton-conducting membranes, *Polymer* (2015), doi: 10.1016/j.polymer.2015.03.071.

This is a PDF file of an unedited manuscript that has been accepted for publication. As a service to our customers we are providing this early version of the manuscript. The manuscript will undergo copyediting, typesetting, and review of the resulting proof before it is published in its final form. Please note that during the production process errors may be discovered which could affect the content, and all legal disclaimers that apply to the journal pertain.



**Columnar Liquid Crystalline Polyglycidol derivatives: a novel alternative for proton-conducting membranes**

Xavier Montané<sup>1</sup>, Suryakant Vilasrao Bhosale<sup>1</sup>, José Antonio Reina<sup>1</sup>, Marta Giamberini<sup>2\*</sup>

<sup>1</sup>Departament de Química Analítica i Química Orgànica, Universitat Rovira i Virgili, Carrer Marcel·li Domingo s/n, Campus Sescelades, 43007 Tarragona, Spain

<sup>2</sup>Departament de Enginyeria Química, Universitat Rovira i Virgili, Av. Països Catalans, 26 Campus Sescelades, 43007 Tarragona, Spain

\*Correspondence to: M. Giamberini (E-mail: [marta.giamberini@urv.cat](mailto:marta.giamberini@urv.cat))

**ABSTRACT**

A family of self-assembling LC columnar polyethers was prepared by chemical modification of linear polyglycidol with a polymerization degree equal to 20, with the dendron 3,4,5-tris[4-(n-dodecan-1-yloxy)benzyloxy]benzoic acid by Steglich esterification. The modification degrees of the resulting LC polyethers ranged between 8 and 43%. All the obtained copolymers exhibited LC behavior and the higher the modification degree, the higher the clearing range, as expected. Mesophase self-assembling depended on the amount of dendrons introduced: in the case of modification degree ranging around 10%, the copolymers exhibited lamellar columnar structure, while for the highest modification degrees, hexagonal columnar mesophase resulted; in the case of intermediate degree of modification, the copolymers exhibited a rectangular columnar mesophase. Oriented membranes could be prepared from modified polyglycidol with different modification degrees and showed promising proton permeability values. Therefore, these materials are proposed as interesting candidates for proton transport materials.

**Keywords:** polyglycidol; liquid-crystalline polymers (LCP); ionic channel; columnar phases; dendrons; biomimetic; supramolecular structures.

## 1. Introduction

Most research in the field of proton conductivity has been devoted by the materials science community in the last thirty years, mainly for the development of new proton-conducting materials to be used in electrochemical cells (e.g. fuel cells, batteries, sensors). In this field, perfluorosulfonic acid (PFSA) membranes, such as Nafion<sup>®</sup> (marketed by DuPont), represent the benchmark materials for their proton-conducting properties [1]. However, these materials exhibit serious drawbacks, such as the need of controlling water management, relative affinity of methanol and water in direct methanol fuel cells (DMFCs), mechanical, thermal and oxidative stability, high cost and environmental inadaptability. For this reason, more than 200 patents and papers have been recently published on the preparation of new proton-conducting membranes [2-5]. An alternative approach is to design materials containing ion transport channels, in which the channels localize the permeation path and simultaneously protect the transport process against the environment, like an ion-transporting molecular cable [6-9].

Percec and coworkers have comprehensively investigated the self-organization of supramolecular monodendrons and styrene-, methacrylate-, or oxazoline-based polymers for the design of ion-active nanostructured supramolecular systems [10-14].

Columnar structures were also obtained for liquid crystalline block copolymers based on dendronized polymers from poly(ethyleneglycol), polystyrene or polymethacrylate (PMA) [15-17]. In this case, the combination of dendrimer structure with the characteristic microphase separation of traditional linear block copolymers, gives rise to macromolecular architectures which can find several applications such as optical storage materials or membranes. Successful perpendicular or parallel orientation

of cylindrical nanodomains has recently been obtained for a liquid crystalline block copolymer based on poly(ethylene oxide) and PMA-bearing azobenzene mesogen side chains, by air-anchoring or surface effect, respectively [18].

In our previous studies [19-21], we reported the chemical modification of poly(epichlorohydrin) (PECH) and poly(epichlorohydrin-co-ethylene oxide) [P(ECH-co-EO)] with tapered mesogenic groups to yield high-molecular-weight polyethers with different degrees of modification. As we reported, these polymers self-assemble into a columnar structure, due to an exo-recognition of the side-chain dendrons. In the resulting structure, the polyether main chain forms a channel in the inner part of the columns, while the hydrophobic side-chain dendrons lie in the outer part. The presence of the polar ether linkages in the inner channel favors the interaction with proton and other cations, in the same way as crown ethers would do [22]. For this reason, the inner polyether chain could work as an ion channel. Satisfactory orientation of the polymer was achieved by sandwiching the polymer solution between a water layer and a wet glass layer to induce unfavorable surface interactions between the outer, hydrophobic portion of the columns and their surroundings. The presence of oriented channels in the polymeric membrane resulted in remarkable proton permeability, around  $2 \cdot 10^{-6} \text{ cm}^2 \text{ s}^{-1}$ , comparable to that of Nafion<sup>®</sup> N117 [23]. However, the procedure used to prepare the oriented membranes had poor reproducibility.

Another drawback which could be exhibited by polyethers obtained out of modified PECH and [P(ECH-co-EO)], lies in the presence of remaining chlorine atoms in the modified polymers, which can lead to long-term development of radical reactions that could alter polymer structure and accelerate its degradation. Polyols like linear polyglycidol (LPG) can be other suitable polyether candidates which can be modified

with 3,4,5-tris[4-(n-dodecan-1-yloxy)benzyloxy]benzoic acid in order to obtain liquid crystalline columnar polyethers, which do not contain chlorine. In this paper, we investigated the modification of LPG using carbodiimide mediated Steglich esterification between free hydroxyl groups of the linear polyglycidol and carboxylic groups of the dendron under different conditions. The use of a lower molecular weight precursor polymer, could lead to systems that can be more easily oriented: therefore, chemical modification was performed on a relatively low molecular weight LPG. In this way, we also intended to test the performances of a lower molecular weight modified polyether as far as orientation and transport are concerned. Modified LPGs were subsequently studied in terms of liquid crystalline behaviour. It was found that modified LPGs are showing different mesophases like lamellar columnar, rectangular columnar (distorted hexagonal) and hexagonal columnar depending on the degree of modification, the higher the number of dendrons, the more ordered the mesophase. Finally, we prepared oriented membranes based on selected copolymers, having three different modification degrees. In this case, membrane orientation was achieved by means of a simpler and reproducible thermal treatment on fluorinated ethylene propylene sheet support. The obtained membranes exhibited promising proton permeabilities, in one case comparable to that of Nafion® and negligible water uptake. Therefore, transport can be attributed to the presence of the oriented channels.

## 2. Experimental

### 2.1 Materials

All the chemicals were purchased from Sigma–Aldrich, while all solvents were purchased from Scharlab. Diglyme (bis(2-methoxyethyl) ether), *p*-toluenesulfonic acid monohydrate (*TsOH*, 98.5%), potassium tert-butoxide (1M solution in THF), *N,N'*-

Dicyclohexylcarbodiimide (DCC, 99%), 4-dimethylaminopyridine (DMAP,  $\geq 99\%$ ), trimethylolpropane (TMP) (97%) and potassium methylate solution (25% v/v in methanol) were used as received. Glycidol (96%) was distilled under reduced pressure and stored over molecular sieves at 2-5°C. Dimethylformamide (DMF, 99%) and dioxane were dried before use.

3,4,5-tris[4-(n-dodecan-1-yloxy)benzyloxy]benzoic acid (compound **D**) was synthesized as previously reported [24]. Yield: 93%.

### 2.1.1 Synthesis of linear polyglycidol (LPG) (Scheme S1)

Linear poly[(1-ethoxyethyl)glycidyl ether] was prepared from (1-ethoxyethyl)glycidyl ether according to Schmitz et al [25]. Linear polyglycidol was prepared by subsequent removal of the acetal protecting groups of [linear (1-ethoxyethyl)glycidyl ether] under acidic hydrolysis conditions. Yield: 78%. Degree of polymerization (DP) = 20.

$^1\text{H NMR}$  ( $^d\text{DMSO}$ , TMS,  $\delta$ , ppm): = 7.3-7.1 (m, 3H), 4.5 (s, 1H), 3.7-3.3 (m, 7H), 2.6 (t, 2H), 1.7 (q, 2H).

$^{13}\text{C NMR}$  ( $^d\text{DMSO}$ , TMS,  $\delta$ , ppm): 145-125 (Aryl), 81.1 ( $\text{CH}_2\text{CHOCH}_2$ ), 74-70 ( $\text{ArCH}_2\text{CH}_2\text{CH}_2$ ,  $\text{CH}_2\text{OCH}_2\text{CH}$ ,  $\text{OCH}_2\text{CHOH}$ ), 64.8 ( $\text{CHCH}_2\text{OH}$ ), 61.1 ( $\text{OCH}_2\text{CHOCH}_2\text{OH}$ ), 32-31 ( $\text{ArCH}_2\text{CH}_2$ ,  $\text{ArCH}_2\text{CH}_2$ ).

### 2.1.2 Modification of linear polyglycidol (Scheme 1)

The linear polyglycidol was successfully modified by compound **D** using carbodiimide mediated Steglich esterification [26] between the free hydroxyl groups of the linear polyglycidol and carboxylic group of **D**:

In three necked round bottom flask, solution of **D** (2 g, 2 mmol) was prepared by dissolving into dry DMF (5 mL). Stoichiometric amounts of DCC and DMAP at 0°C

were allowed to stir for 30 min in an Ar atmosphere. The necessary amount of linear polyglycidol was dissolved into dry DMF (5 ml) and added dropwise to the above reaction mixture. The reaction mixture was allowed to stir for 2 days at room temperature under Ar atmosphere. Afterwards, the reaction mixture was precipitated in 500 ml of methanol. Precipitated product was dissolved into THF and re-precipitated in 500 ml methanol. This precipitation was repeated for 5 times, in order to remove DCC, DMAP, free acid and other impurities. After precipitation, the modified polymer was collected and dried at 40°C *in vacuo* for 48 hours.

Different degrees of modifications and corresponding yields are given in Table 1.

### 2.1.3 Membranes preparation

Membranes were prepared by immersion precipitation process, in which a homogeneous polymer solution in THF (30% w/w) was cast on a FEP (fluorinated ethylene propylene) sheet support and immersed in a bath of Milli-Q water. The solvent diffused into the precipitation bath, while the non-solvent (water) diffused into the cast film. After a time in which the solvent and the non-solvent were exchanged, the polymer solution (wet film) became thermodynamically unstable and demixing took place. Finally, a solid polymer membrane was formed with an asymmetric structure. Afterwards, the membrane was dried overnight at room temperature and subsequently used for baking process. The polymer membrane along with FEP sheet was mounted on a hot stage (Linkam TP92) and it was heated above the clearing temperature; then it was allowed to cool slowly (0.5°C/min) down to room temperature. After the baking process, the membrane was kept at room temperature for approximately 1 hour and then it was separated from the FEP sheet and obtained as an intact, uniform membrane with

thickness around 300  $\mu\text{m}$ . Membranes were in their rubbery state at room temperature (see Table 3) and they flowed above their clearing temperature.

## 2.2 Characterization and Measurements

$^1\text{H}$  NMR and  $^{13}\text{C}$  NMR spectra were recorded at 400 and 100.4 MHz, respectively, on a Varian Gemini 400 spectrometer with proton noise decoupling for  $^{13}\text{C}$  NMR. The  $^{13}\text{C}$  NMR spectra of the polymers were recorded at 30°C, with a flip angle of 45°, and the number of transients ranged from 20,000 to 40,000 with 10–20% (w/v) sample solutions in  $\text{CDCl}_3$ . The central peak of  $\text{CDCl}_3$  was taken as the reference, and the chemical shifts were given in parts per million from TMS (Tetramethylsilane) with the appropriate shift conversions.

Thermal transitions were detected with a Mettler–Toledo differential scanning calorimeter mod. 822 in dynamic mode at a heating or cooling rate of 10°C/min. Nitrogen was used as the purge gas. The calorimeter was calibrated with an indium standard (heat flow calibration) and an indium–lead–zinc standard (temperature calibration).

Clearing temperatures and liquid crystalline mesophases were investigated by polarized optical microscopy (POM); textures of the samples were observed with an Axiolab Zeiss optical microscope equipped with a Linkam TP92 hot stage.

Densities were determined by gas pycnometry using Micromeritics AccuPyc 1330 machine at 30°C.

Average molecular weights were determined in THF by size exclusion chromatography (SEC); analyses were carried out with an Agilent 1200 series system with PLgel 3  $\mu\text{m}$  MIXED-E, PLgel 5  $\mu\text{m}$  MIXED-D, and PLgel 20  $\mu\text{m}$  MIXED-A

columns in series, and equipped with an Agilent 1100 series refractive-index detector. Calibration curves were based on polystyrene standards having low polydispersities. THF was used as an eluent at a flow rate of 1.0 mL/min, the sample concentrations were 5-10 mg/mL, and injection volumes of 100  $\mu$ L were used.

For X-ray experiments, two different diffractometers were used depending on the  $2\theta$  range investigated:

For low  $2\theta$  range: XRD measurements were performed with a Bruker-AXS D8-Discover diffractometer equipped with parallel incident beam (Göbel mirror), vertical  $\theta$ - $\theta$  goniometer, XYZ motorized stage and with a GADDS (General Area Detector Diffraction System). Samples were placed directly on to a low background Si(510) sample holder for reflection analysis. An X-ray collimator system close-to-the-sample allows to analyze areas of 500  $\mu$ m. The X-ray diffractometer was operated at 40 kV and 40 mA to generate  $\text{Cu}_{k\alpha}$  radiation. The GADDS detector was a HI-STAR (multiwire proportional counter of 30x30 cm with a 1024x1024 pixel) placed at 30cm from the sample. The X-ray beam hit the sample at 0.5° of incidence. The collected frame (2D XRD pattern) covers a range from 0.9 up to 9.2°  $2\theta$ . The diffracted X-ray beam travels through a He beam path (SAXS attachment) to reduce the air scattering at low angles. The direct X-ray beam is stopped by a beam stop placed directly on the detector face. The exposition time was of 300s per frame. The resulting frames were both radially integrated to obtain a  $2\theta$  diffractogram and  $2\theta$  integrated to obtain an azimuthal intensity plot.

For medium  $2\theta$  range: XRD measurements were performed with a Siemens D5000 diffractometer (Bragg-Brentano parafocusing geometry and vertical  $\theta$ - $\theta$  goniometer) fitted with a curved graphite diffracted-beam monochromator, incident and diffracted-beam Soller slits, a 0.06° receiving slit and scintillation counter as a detector.

Samples were placed directly on to a low background Si(510) sample holder for reflection analysis. The X-ray diffractometer was operated at 40 kV and 30 mA to generate  $\text{CuK}_\alpha$  radiation. The angular  $2\theta$  diffraction range was between 1 and  $40^\circ$ . The data were collected with an angular step of  $0.03^\circ$  at 6s per step. In the case of membranes, XRD experiments were performed on both sides and no differences could be detected.

The thickness of the membranes was measured using a micrometer with a sensitivity of 2  $\mu\text{m}$ . The measurements were carried out at various points, and the membranes were found to have constant thickness.

Contact angles of water drops on a membrane surface were measured with a Kruss contact angle instrument (Hamburg, Germany) equipped with a motorized pipet (Matrix Technology, Nashua, NH) and deionized water as the probe liquid. The contact angle was measured immediately after putting the water drop (3  $\mu\text{L}$ ) on the membrane surface. Measurements were repeated using different areas of the membrane. For each test reported, at least three drops of water were used.

Swelling experiments were performed by soaking the membranes at room temperature in milli-Q water and monitoring the change in membrane weight versus time for 24 h.

Transport experiments were carried out using a Teflon test cell that comprised two compartments, separated by the tested membrane, containing the feed and stripping solutions, respectively. The feed and stripping volumes were 200 ml and the effective membrane area was  $0.86 \text{ cm}^2$ . For the proton transport experiments, the initial feed solution was 0.1 M HCl aqueous solution and the stripping solution was 0.1 M NaCl aqueous solution. The pH of the stripping solution was measured every 30 s by a Crison

MM 40 Multimeter. Prior to the proton transport experiments, membranes were conditioned in 0.1 M NaCl aqueous solution for 15 min.

Under steady-state conditions, proton flux was calculated by Fick's First Law:

$$J = \frac{P\Delta C}{l} \cdot 10^{-3} \quad (1)$$

where  $l$  (cm) is the membrane thickness and  $\Delta C$  is the difference in concentration ( $\text{mol l}^{-1}$ ) between the initial feed solution ( $C_0$ ) and the final stripping solution. In our experimental conditions,  $C_0$  was much greater than the final stripping concentration, so we considered  $\Delta C \sim C_0$ .

$P$  is the proton permeability ( $\text{cm}^2 \text{s}^{-1}$ ), defined as:

$$P = DS \quad (2)$$

where  $D$  is the proton diffusion coefficient and  $S$  is the sorption equilibrium parameter.

The flux is related to the permeability coefficient  $p$  ( $\text{cm s}^{-1}$ ), as:

$$J = pC_0 \quad (3)$$

$$P = pl \quad (4)$$

The permeability coefficient, can be described by the following equation:[27]

$$-\ln \frac{C_f}{C_0} = \frac{Ap}{V_f} t \quad (5)$$

where  $C_0$  ( $\text{mol l}^{-1}$ ) is the initial concentration of the feed solution and  $C_f$  ( $\text{mol l}^{-1}$ ) is the feed concentration calculated from the stripping solution at time  $t$  (s):

$$C_f = C_0 - C_s \quad (6)$$

$V_f$  is the feed volume (mL) and  $A$  is the actual membrane area ( $\text{cm}^2$ ).

We calculated the proton permeabilities in accordance with the above equations. Data were fitted according to equation (5) in the time range  $(1.2-500) \times 10^3$  s, depending on the system under investigation.

### 3. Results and discussion

#### 3.1 Synthesis of linear polyglycidol (LPG)

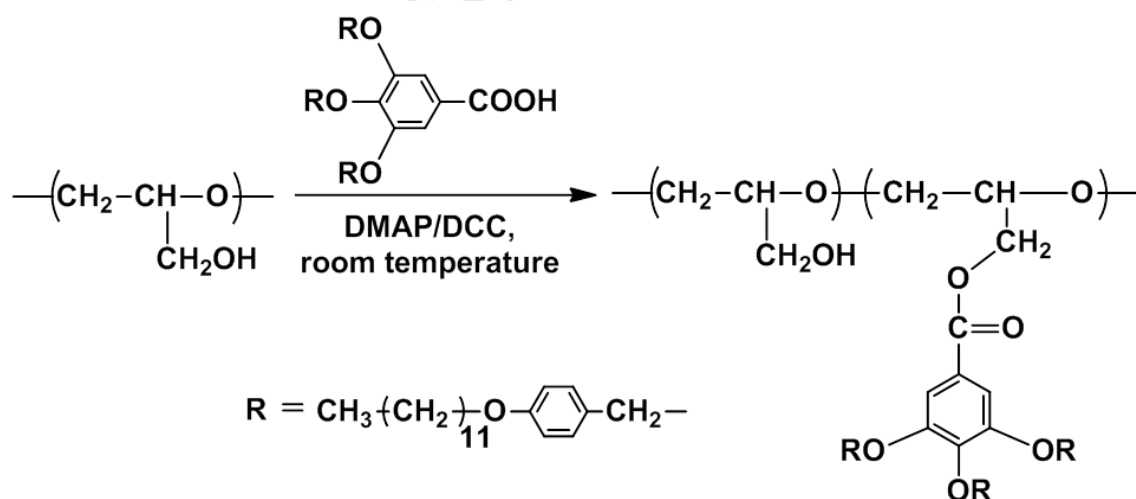
As explained in the experimental part and shown in Scheme S1, (1-ethoxyethyl)glycidyl ether was first synthesized from glycidol according to Fitton et al. [28]; then, linear poly[(1-ethoxyethyl)glycidyl ether] was prepared from (1-ethoxyethyl)glycidyl ether according to Schmitz et al. [25]. Finally, LPG was prepared by subsequent removal of the acetal protecting groups.

The structure of the obtained linear polyglycidol was confirmed by  $^1\text{H}$  and  $^{13}\text{C}$  NMR techniques as shown in Figure S1 and S2, respectively. The presence of the aromatic ring as a head group, allowed calculating the degree of polymerization (DP) from  $^1\text{H}$  NMR spectra, by comparing the integrated areas of the peaks coming from aromatic, aliphatic and alcoholic protons as shown in Figure S1. DP resulted equal to 20.

### 3.2 Modification of LPG

The Steglich esterification represents one of the most versatile esterification methods, which take advantages of *N,N'*-dicyclohexylcarbodiimide (DCC) as a promoter [26]. Although stoichiometric dosage of this reagent, or more, is necessary, this procedure enjoys various advantages. The reaction usually proceeds at room temperature, and the conditions are so mild that substrates with various functional groups can be employed. The reaction is not sensitive to steric hindrance of the reactants, allowing production of esters of tertiary alcohols. As such, a wide range of applications have been achieved in the field of natural products, peptides, nucleotides, etc. however, unfortunately this procedure has some drawbacks: yields are not always high, and undesirable *N*-acylureas are occasionally formed. These drawbacks can be overcome by addition of strong acids such as *p*-toluenesulfonic acid [29]. Alternatively, addition of a catalytic amount of *p*-aminopyridines is more effective [30, 31].

In this way, we applied Steglich esterification in chemical modification of LPG (Scheme 1).



**Scheme 1** Chemical modification of linear polyglycidol.

In case of LPG, we studied this chemical modification under different reaction conditions, which are given in Table 1 along with their corresponding degree of modification and product yields.

**Table 1** Modification degrees and yields obtained in modification of LPG

Sample	RCOOH (mmol) <sup>a</sup>	-OH/RCOOH	Time (days)	T (°C)	Modification degree (%) <sup>b</sup>	Yield (%)	
c {	LPG1	2	1:0.3	2	25	8	61
	LPG2	2	1:0.5	2	25	23	70
	LPG3	2	1:0.7	2	25	27	68
	LPG4	2	1:1	2	25	39	81
	LPG5	2	1:1.25	2	25	43	87
d {	LPG6	2	1:1	7	25	42	79
	LPG7	2	1:1	2	40	40	75
	LPG8	2	1:1	2	80	11	65

<sup>a</sup> Stoichiometric amounts of DCC and DMAP in each case

<sup>b</sup> Average value determined by <sup>1</sup>H NMR

<sup>c</sup> Series 1

<sup>d</sup> Series 2

In most cases this esterification was carried out at room temperature, since the side product N-acylurea formation is less likely at lower temperatures; in other words, high temperatures favor the formation of side products and are therefore expected to reduce modification degrees correspondingly.

We considered products LPG1 to LPG5 as series 1 and from LPG6 to LPG8 as series 2. In case of series 1, only the -OH/ROOH molar ratio was varied, while there was no change in reaction time and temperature. It can be seen that in this case the degree of modification increased on increasing the molar ratio; finally, we got 43% degree of modification in case of LPG5.

In case of series 2, we studied the effect of increase in reaction time and temperature on degree of modification. However, the degree of modification could not be increased with increasing reaction time up to 7 days, as it can be seen in case of LPG6. As far as reaction temperature is concerned, an increase up to 40°C did not affect the reaction since a degree of modification of 40% was reached in the case of LPG7; on the other hand, the degree of modification was significantly decreased up to 11% when the reaction was performed at 80°C, as in the case of LPG8.

Therefore, we supposed a modification plateau of 43%, which could not be further increased by raising reaction time and temperature. Reaction yield could not be improved beyond 87% (LPG5); however, one should take into account that, in order to get rid of DMAP and DCC, several precipitations were required which caused loss of product and inevitably turned into low product yield.

The structure of the copolymers was characterized by NMR spectroscopy. Figure 1 reports the  $^1\text{H}$  NMR spectrum in  $\text{CDCl}_3$  of modified LPG1 as an example.

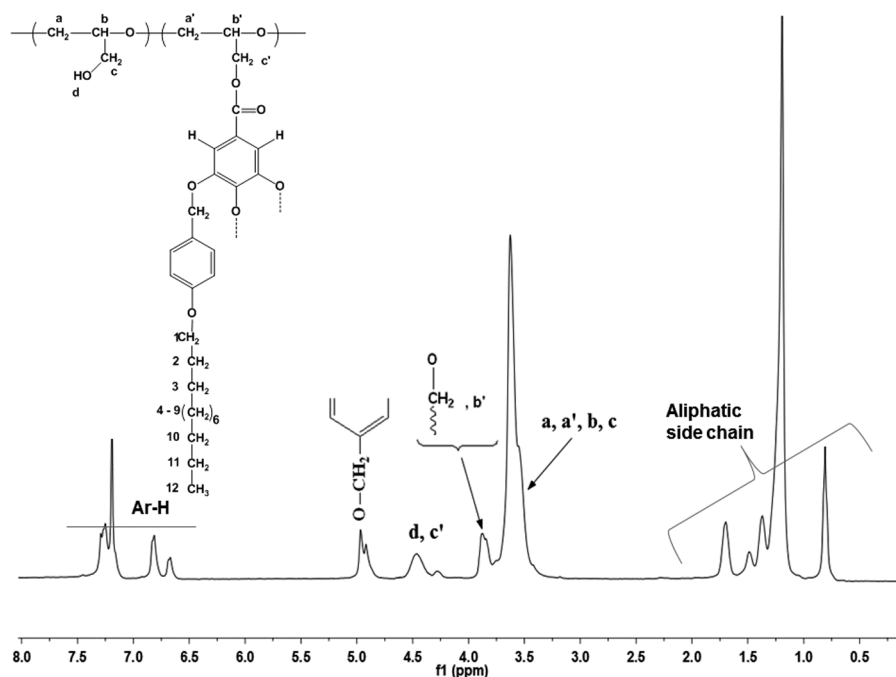


**Figure 1.**  $^1\text{H}$  NMR spectrum of modified LPG1 in  $\text{CDCl}_3$

All  $^1\text{H}$  NMR spectra are characterized by broad signals in three regions. The aromatic region shows three signals at 7.2, 6.8, and 6.7 ppm. Considering the relative integration areas and by comparison with the spectrum of methyl 3,4,5-tris(n-dodecan-1-yloxy)benzoate, the signal at 7.2 (8H) can be assigned to the protons of the benzoate group plus the aromatic protons ortho to the benzylic carbon  $-\text{CH}_2\text{O}-$ . The signals at 6.8 and 6.6 ppm (4H+2H) correspond to the aromatic protons meta to the benzylic carbon  $-\text{CH}_2\text{O}-$  of the lateral and central alkyloxybenzyloxy substituents respectively. The characteristic signals, corresponding to most protons of the dodecyloxy alkyl chains in the dendron, can be observed in the high-field region at 1.7, 1.4, 1.3, 1.2, and 0.8 ppm. In the region between 5 and 3.4 ppm five signals can be observed: the two signals at 4.4 and 4.3 ppm correspond to the methylenic protons  $c'$  in the modified monomeric unit; in this region, also signals coming from the free  $-\text{OH}$  groups are overlapped. The signal at 3.9 ppm corresponds to the methylene attached to the oxygen in the alkyl chains of the

mesogenic unit and to methinic proton b'. The broad signal between 3.8 and 3.4 ppm corresponds to the methylenic and methinic protons a, a', b, and c in the modified and unmodified monomeric units. Finally, the signal centered at 4.9 ppm can be assigned to the benzylic methylenes of the dodecyloxybenzyloxy substituent.

Figure 2 shows the  $^{13}\text{C}$  NMR spectrum 1,1,2,2-tetrachloroethane-d<sub>2</sub> of modified LPG1 with the corresponding assignments.

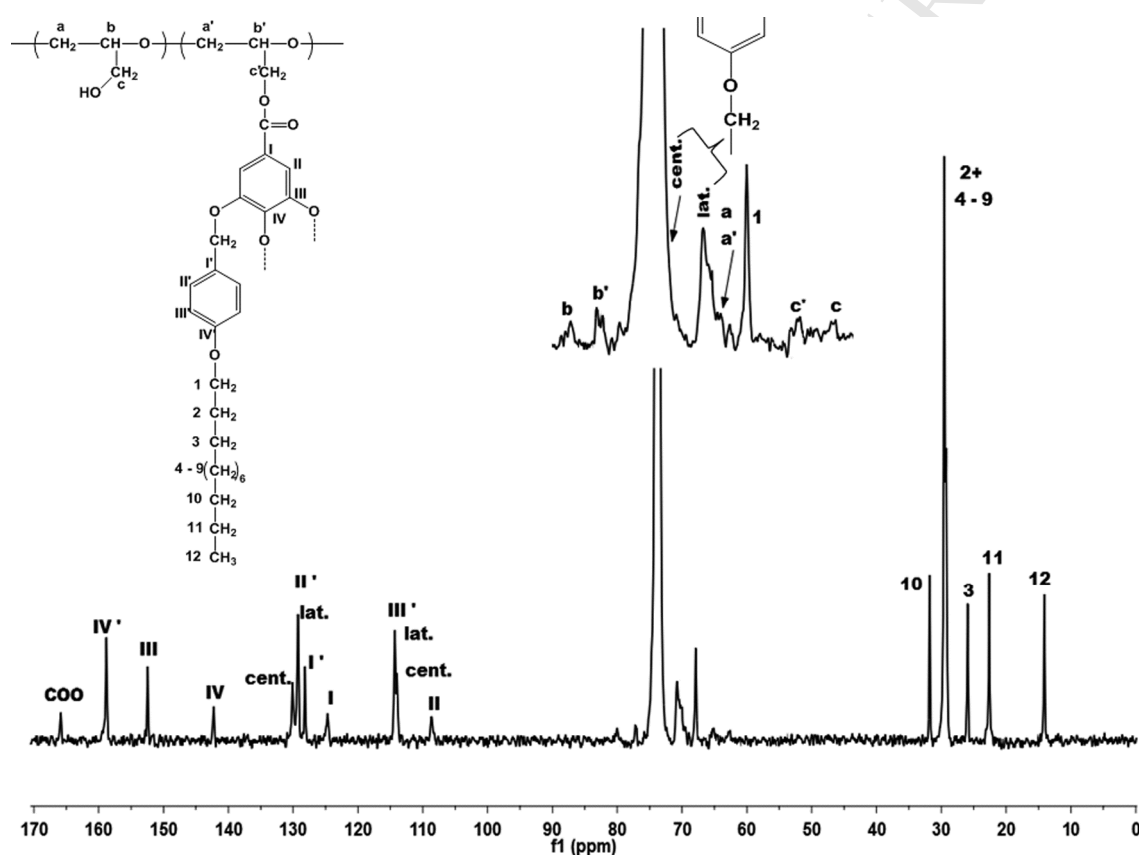


**Figure 2.**  $^{13}\text{C}$  NMR spectrum of modified LPG1 in 1,1,2,2-Tetrachloroethane-d<sub>2</sub>

The aromatic carbons and the carbonyl carbon appear between 166 and 108 ppm, whereas carbons 2–12 of the aliphatic alkyl chains appear in the region between 32 and 14 ppm. The carbons of the backbone appear in the central region of the spectrum. The methine and side methylenic carbons of the modified and unmodified

monomeric units appear at different chemical shifts. Thus, b and b' appear at 80.6 and 77.4 ppm, while c and c' appear at 62.2 and 64.4 ppm respectively. The carbons a and a' appear overlapped at 69.5 ppm. Carbon 1 of the alkyl chains appears as a sharp peak at 67.8 ppm. The chemical shifts of the benzylic methylenes depend on their relative position in the benzoate ring: those in position 3 and 5 appear at 71.1 ppm, whereas the same carbon in position 4 appears overlapped with peaks coming from 1,1,2,2-tetrachloroethane-d<sub>2</sub>.

The degree of modification of modified polymer was calculated by <sup>1</sup>H NMR spectra by comparing the areas of the aromatic peaks between 7.4 and 6.6 ppm and the benzylic proton signal at 4.9 ppm with the broad signal between 3.8 and 3.4 ppm.

Molecular weights and polydispersities of LPG derivatives determined by SEC are reported in Table 2. Molecular weights increased with modification degree. In general terms, density values (Table 2) did not exhibit appreciable variation; slightly higher values were found in the case of LPG5, LPG6 and LPG7, which also showed higher polydispersities.

**Table 2** Average molecular weights and densities of the modified LPG

Sample	Modification degree (%)	$M_n \cdot 10^{-3b}$	$M_w \cdot 10^{-3b}$	$M_w/M_n^b$	$\rho$ (g/cm <sup>3</sup> ) <sup>c</sup>
LPG1	8	2.70	3.19	1.18	1.07
LPG2	23	4.79	6.57	1.37	1.07
LPG3	27	5.16	7.34	1.42	1.08
LPG4	39	7.36	10.87	1.47	1.08
LPG5	43	7.62	12.76	1.62	1.17
LPG6	42	7.52	11.46	1.52	1.17
LPG7	40	7.11	10.93	1.53	1.17
LPG8	11	2.93	3.57	1.21	1.07
LPG <sup>a</sup>	-	1.48 <sup>d</sup>	-	-	1.02

<sup>a</sup> Unmodified linear polyglycidol.

<sup>b</sup> Determined by SEC

<sup>c</sup> Determined at 30<sup>0</sup>C. Error:  $\pm$  3%

<sup>d</sup> Calculated from <sup>1</sup>H NMR

### 3.3 Mesomorphic characterization of modified LPG

Mesomorphic phases were investigated by Differential Scanning Calorimetry (DSC), Polarized Optical Microscopy (POM) and confirmed by X-ray diffraction (XRD). Table 3 shows the clearing temperatures ranges and the glass transition temperatures of the whole LPG series.

**Table 3** Clearing temperature ranges and glass transition temperatures of the modified LPG

Sample	Modification (%)	$T_g$ (°C) <sup>a</sup>	$T_c$ (°C) <sup>b</sup>
<b>LPG</b>	-	-10	-
<b>LPG1</b>	8	-10	32-35
<b>LPG2</b>	23	-30	71-75
<b>LPG3</b>	27	-32	79-84
<b>LPG4</b>	39	-27	97-101
<b>LPG5</b>	43	-16	116-120
<b>LPG6</b>	42	-21	95-98
<b>LPG7</b>	40	-13	95-99
<b>LPG8</b>	11	-20	49-52

<sup>a</sup> Determined by DSC second heating scan

<sup>b</sup> Determined by DSC second heating scan and POM

The liquid crystalline textures of LPG samples were observed by POM after annealing the samples for two hours at a temperature slightly lower than their respective clearing temperatures, in order to favor the growth of the liquid crystalline domains. POM images of both series are shown in Figure 3.

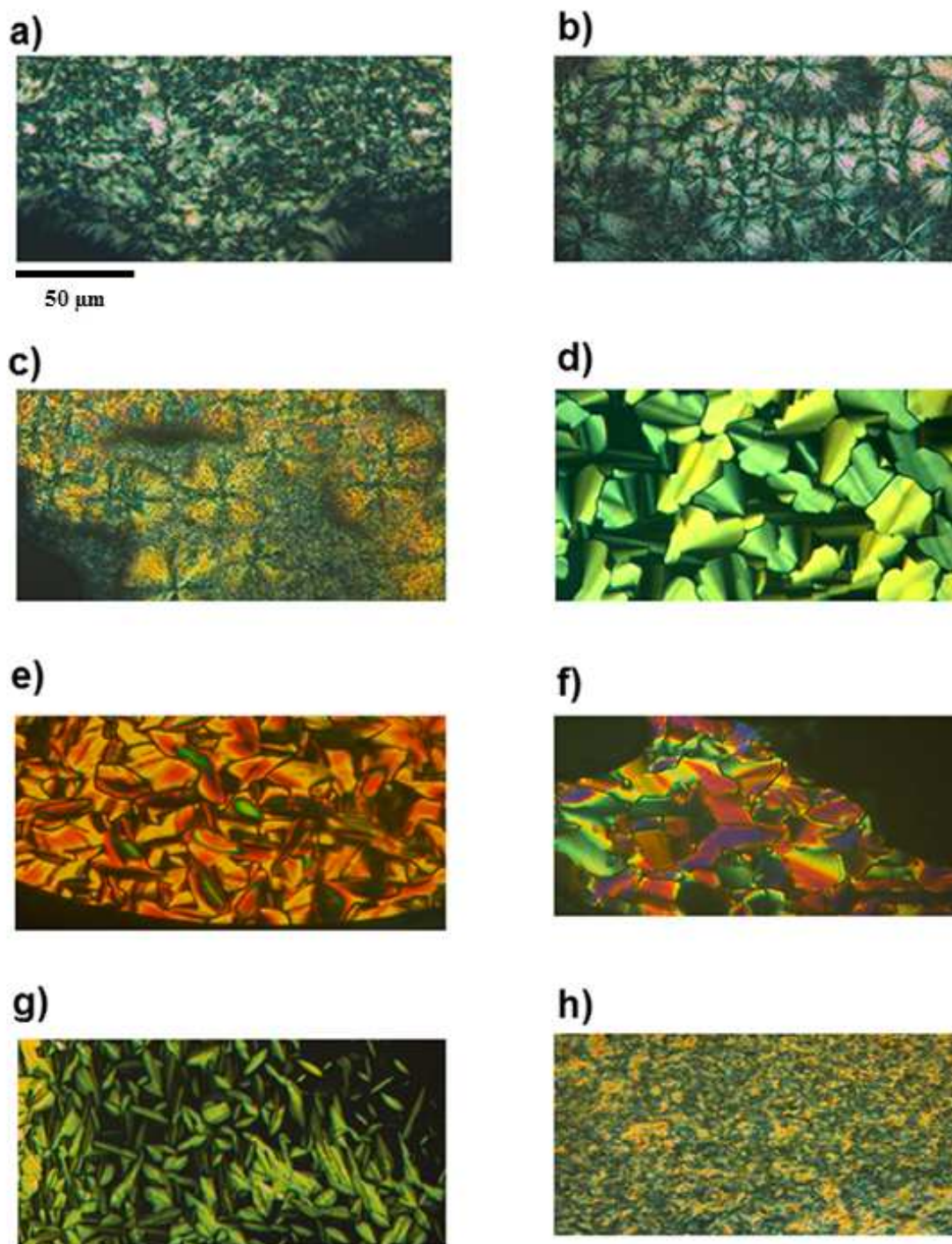


**Figure 3.** Optical micrographics between crossed polars of (sample, modification degree, test temperature: a) LPG1, 8%, 30°C; b) LPG2, 23%, 69°C; c) LPG3, 27%, 79°C; d) LPG4, 39%, 97°C; e) LPG5, 43%, 116°C; f) LPG6, 42%, 94°C; g) LPG7, 40%, 93°C; and h) LPG8, 11%, 47°C.

A typical broken fan-shaped texture could be seen in case of LPG2 - LPG7 samples, whose modification degrees ranged between 20 and 40% approximately. At variance, LPG1 and LPG8, with modification degrees around 10%, exhibited a texture which resembled smectic bâtonnets.

In order to assign their mesophases, LPG1, LPG2, LPG3 and LPG4 were studied by XRD. LPG5-LPG7 have modification degrees quite close to LPG4 and, in the case of LPG6 and LPG7, the clearing range was also similar to LPG4. Therefore, we considered reasonable to extend the results from XRD experiments on LPG4 also to LPG5-LPG7. In case of LPG8, similar texture to LPG1 was observed by POM, but the glass transition temperature and the clearing temperature range resulted quite different, so we decided to characterize it as well. Summing up, only samples from LPG1 to LPG4 and LPG8 were analyzed by XRD. The results from XRD are summarized in Table 4.

**Table 4** X-ray diffraction data of LPG copolymers at room temperature

Sample	Modification degree (%)	$d_{\text{exp}}$ (Å)	hkl	Mesophase <sup>b</sup>	Lattice constants (Å)
LPG1	8	42.0	100	<i>Col<sub>L</sub></i>	a= 42.0
		4.4 (b) <sup>a</sup>	001		
LPG8	11	40.1	100	<i>Col<sub>r</sub></i>	a=40.1 b= 25.0
		25.0	010		
		13.8	020		
		4.3 (b) <sup>a</sup>	001		
LPG8OM <sup>c</sup>	11	40.3	100	<i>Col<sub>r</sub></i>	a=40.3 b= 26.0
		26.0	010		
		13.1	020		
		4.3 (b) <sup>a</sup>	001		
LPG2	23	41.1	100	<i>Col<sub>r</sub></i>	a=41.1 b= 27.3
		27.3	010		
		13.5	020		
		4.4 (b) <sup>a</sup>	001		
LPG2 OM <sup>c</sup>	23	40.0	100	<i>Col<sub>L</sub></i>	a= 40.0
		4.4 (b) <sup>a</sup>	001		
LPG3	27	41.0	100	<i>Col<sub>h</sub></i>	a=b=47.3
		23.8	110		
		4.4 (b) <sup>a</sup>	001		
LPG4	39	46.4	100	<i>Col<sub>h</sub></i>	a=b=53.6
		26.3	110		
		23.5	200		
		4.6 (b) <sup>a</sup>	001		
LPG4 OM <sup>c</sup>	39	36.5	100	<i>Col<sub>h</sub></i>	a=b=42.1
		21.8	110		
		18.1	200		
		4.6 (b) <sup>a</sup>	001		
		31.4	100		
		25.6	010	a=31.4 b= 25.6	
		15.5	200		
		13.1	020		
		4.6 (b) <sup>a</sup>	001		

<sup>a</sup> (b): broad halo<sup>b</sup> *Col<sub>L</sub>*: lamellar columnar, *Col<sub>r</sub>*: rectangular columnar, *Col<sub>h</sub>*: hexagonal columnar<sup>c</sup> Oriented membrane obtained by immersion precipitation + baking process

The intensity vs.  $2\theta$  graph of LPG1 copolymer is shown in Figure S3. Only two signals are evident, a sharp reflection at  $2\theta=2.1^\circ$ , corresponding to a d-spacing of 42.0 Å, and broad halo at  $2\theta$  around  $20^\circ$ , giving a d-spacing of 4.4 Å. This pattern is compatible with a smectic as well as with a lamellar columnar mesophase ( $Col_L$ ); however, the characterization previously performed on the systems obtained out of PECH and [P(ECH-co-EO)] [18] suggested the existence of  $Col_L$  mesophase, the sharp reflection corresponding to the interlamellar distance, while the halo to the distance between adjacent dendrons.

XRD patterns of samples LPG2 and LPG3 are shown in Figure S4 and Figure S5, respectively. In the case of LPG2, we could observe three sharp reflections at  $2\theta = 2.1^\circ$ ,  $3.2^\circ$  and  $6.5^\circ$ , corresponding to  $d = 41.1$  Å,  $27.3$  Å and  $13.5$  Å respectively, and a diffuse halo centered round  $2\theta = 20^\circ$ , giving  $d=4.4$  Å. On the other hand, LPG3 showed two sharp reflections at  $2\theta = 2.1^\circ$  and  $3.7^\circ$ , corresponding to  $d = 41.0$  Å and  $23.8$  Å respectively, and a diffuse halo centered round  $2\theta = 20^\circ$ , giving  $d = 4.4$  Å. This last diffraction pattern, which exhibited d-spacings of the sharp reflections in the ratio of  $1:1/\sqrt{3}$  and a diffuse halo at high angle region, confirmed the presence of a hexagonal columnar mesophase ( $Col_h$ ), where the first two sharp reflections correspond to the planes (100) and (110) respectively, while the broad halo is related to (001). Similar conclusions could be drawn from the XRD pattern of sample LPG4, since it showed three sharp reflections corresponding to  $d = 46.4$  Å,  $26.3$  Å and  $23.5$  Å respectively, and a diffuse halo centered round  $d = 4.6$  Å. The d-spacings of the sharp reflections were in the ratio  $1:1/\sqrt{3}:1/2$ , confirming the presence of a hexagonal columnar mesophase ( $Col_h$ ). The XRD pattern of LPG4 is reported in Figure S6.

At variance, the X-ray diffraction pattern of polymer LPG2 was in agreement with the less-symmetrical rectangular columnar mesophase ( $\text{Col}_r$ ). In this case, the sharp reflections at 41.1, 27.3 and 13.5 Å could be assigned to (100), (010) and (020) planes, respectively. It must be noted, that the occurrence of a rectangular columnar mesophase is also compatible with the broken fan shaped texture as observed by POM (Figure 3b). Also in the case of LPG8, whose modification degree was 11%, XRD pattern was compatible with a rectangular columnar mesophase (Table 4). As we have explained, on increasing the modification degree, the LC phase of the modified copolymers changed from lamellar columnar to hexagonal columnar, through an intermediate, less symmetric rectangular columnar. This can be ascribed to the self-assembling of the dendrons (Figure 4): in the case of low modification degrees (LPG1), the  $\pi$ - $\pi$  interaction between the aromatic rings, as well as the inter-digitation of peripheral aliphatic chains is only able to drive the system to lamellar packing (Figure 4a) while, when the modification degree is higher (LPG3 to LPG7), the increased symmetry of the system can induce the assembling of the columns into a hexagonal packing (Figure 4c). In the case of intermediate modification degree (LPG2 and LPG8), columnar organization is not perfectly hexagonal yet and the elliptical shape of the column cross-section gives rise to a rectangular columnar mesophase (Figure 4b).

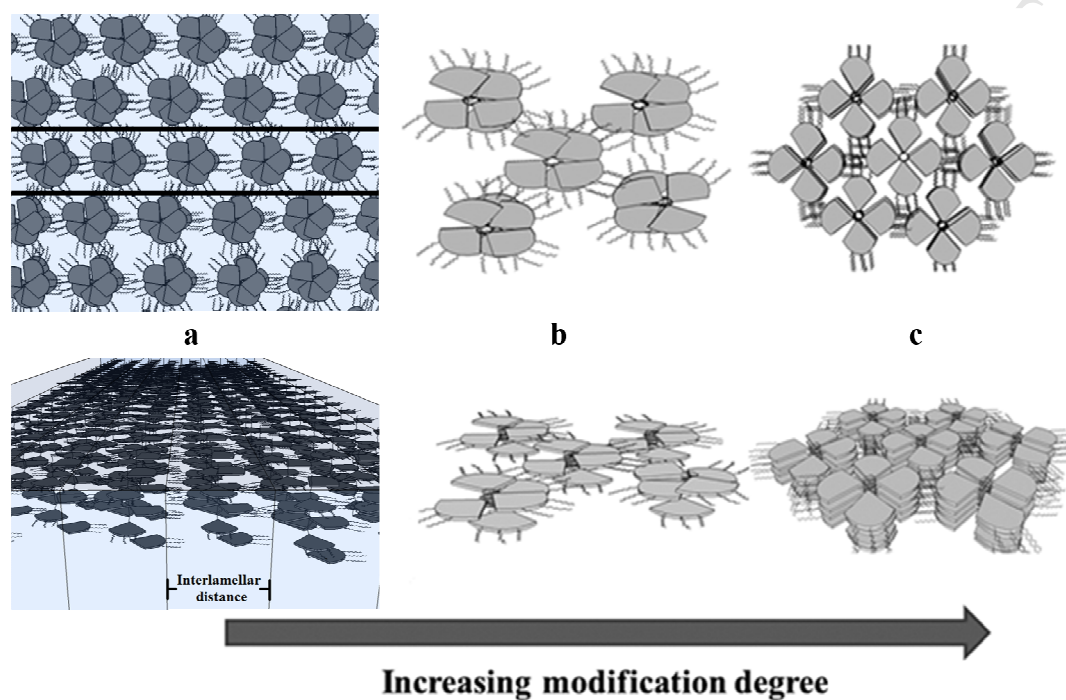


**Figure 4.** Schematic representation of the self-assembly of LPG copolymers on increasing the modification degree; a: lamellar columnar; b: rectangular columnar; c: hexagonal columnar. Top: top views; bottom: side views.

In all cases, the organization of the copolymers into columns can be supposed to lead to the formation of biomimetic ion channels, where the polyether main chain arranges in the inner part of the column.

#### *3.4 Membrane preparation and assessment*

In order to assess the potential of the synthesized copolymers as proton-conducting materials, we prepared oriented membranes out of selected samples. LPG8,

LPG2 and LPG4 were selected as representative of three different increasing modification degrees. In order to get efficient transport, the columns which are expected to work as ion channels should be oriented homeotropically, that is, perpendicularly to the membrane surface.

According to the studies done by Percec et al. [11, 18], it was demonstrated that columnar self-assembling polymers containing tapered groups can be homeotropically oriented when the system is allowed to self-organize during slow cooling on a hydrophobic substrate from the melt into the liquid crystal phases. The dendrons were found to be the structure-directing moieties of the columnar architectures, and  $\pi$ - $\pi$  stacking of aromatic units produces the driving forces responsible for this homeotropic orientation.

Therefore, as mentioned in the experimental part, membranes were first prepared by immersion precipitation process. Then, with the described baking process, we obtained satisfactorily oriented membranes in the homeotropic direction. Previously, the baking process was successfully applied to the preparation of homeotropically oriented membranes based on chemically modified PECH and [P(ECH-co-EO)] [18].

As an example, Figure 5 shows the XRD image of a LPG4 membrane after baking process. The diffraction at  $2\theta = 2.4^\circ$ , which corresponds to  $d_{100} = 36.5 \text{ \AA}$  and to  $a = b = 42.1 \text{ \AA}$ , exhibits orientation in the equatorial plane, which indicates that columns are oriented perpendicularly to the membrane surface to some extent.

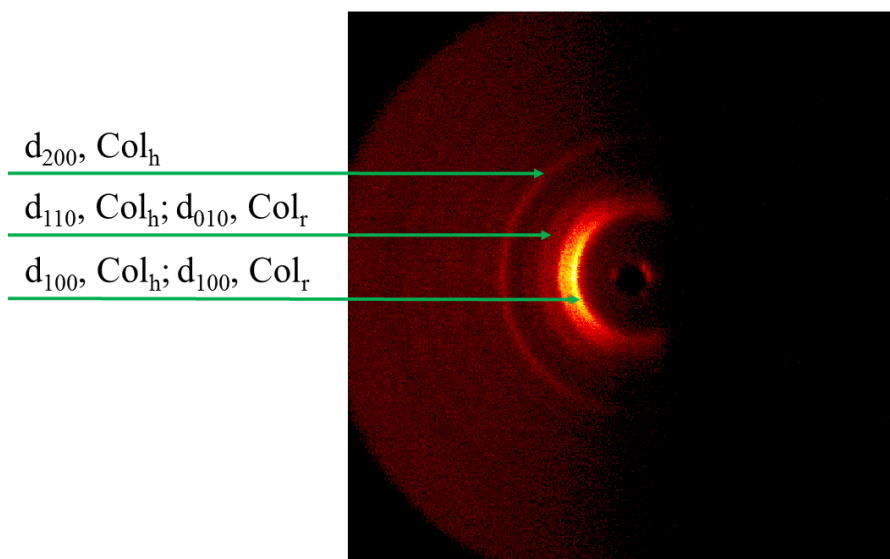


**Figure 5.** XRD pattern of LPG4 oriented membrane at room temperature recorded in reflection mode.

As it can be seen in Table 4, in some cases surface interactions, which are responsible for the orientation process, seem to alter the ordering of LPG copolymers. As a matter of fact, in one case a different mesophase was observed (LPG2), while in another one, coexistence with a new mesophase was put into evidence. (LPG4).

The obtained membranes were also investigated in terms of water contact angle measurement by considering FEP side and air-side, that is, the part which was directly in contact with the FEP support during the baking process, and the other one, on opposite side. The values of contact angles on FEP side are reported in Table 5.

**Table 5** Water contact angles and proton permeabilities of LPG-based oriented membranes

<b>Sample</b>	<b>Water contact angle<sup>a</sup> (°)</b>	<b>Permeability (cm<sup>2</sup> s<sup>-1</sup>)</b>
<b>LPG8</b>	115.8 ± 1.5	2.2 (± 0.5) · 10 <sup>-6</sup>
<b>LPG2</b>	116.4 ± 0.8	3.8 (± 0.1) · 10 <sup>-7</sup>
<b>LPG4</b>	112.3 ± 0.3	1.0 (± 0.3) · 10 <sup>-7</sup>
<b>Nafion<sup>®</sup> N117</b>	94.0 ± 0.9	2.59 (± 0.05) · 10 <sup>-6</sup>

<sup>a</sup> Determined on FEP side

In our case, both sides were found hydrophobic, having similar contact angles. This evidence confirmed that the membranes were homogeneously oriented. Surface hydrophobicity can be ascribed to dominating exposition of tapered groups which represents the hydrophobic part of the polymer: that is, in case of homeotropic orientation, the membrane surface is hydrophobic because of maximum area occupied by well oriented hydrophobic tapered groups.

Proton transport tests were performed on the membrane obtained with LPG8, LPG2 and LPG4. Calculated permeability values are reported in Table 5. The value found for Nafion<sup>®</sup> N117 (2.59 · 10<sup>-6</sup> cm<sup>2</sup>s<sup>-1</sup>) was used as a reference standard in the evaluation of proton permeability of the other materials. Permeabilities of LPG copolymers are comparable to Nafion<sup>®</sup>, while no permeability at all was detected for the samples not previously submitted to the baking process; in the case of LPG8, the calculated value resulted very close to Nafion<sup>®</sup>, being 2.2 (± 0.5) · 10<sup>-6</sup> cm<sup>2</sup>s<sup>-1</sup>. Plots according to equation (5) for Nafion<sup>®</sup> N117 and LPG8 are reported in Figure 6.

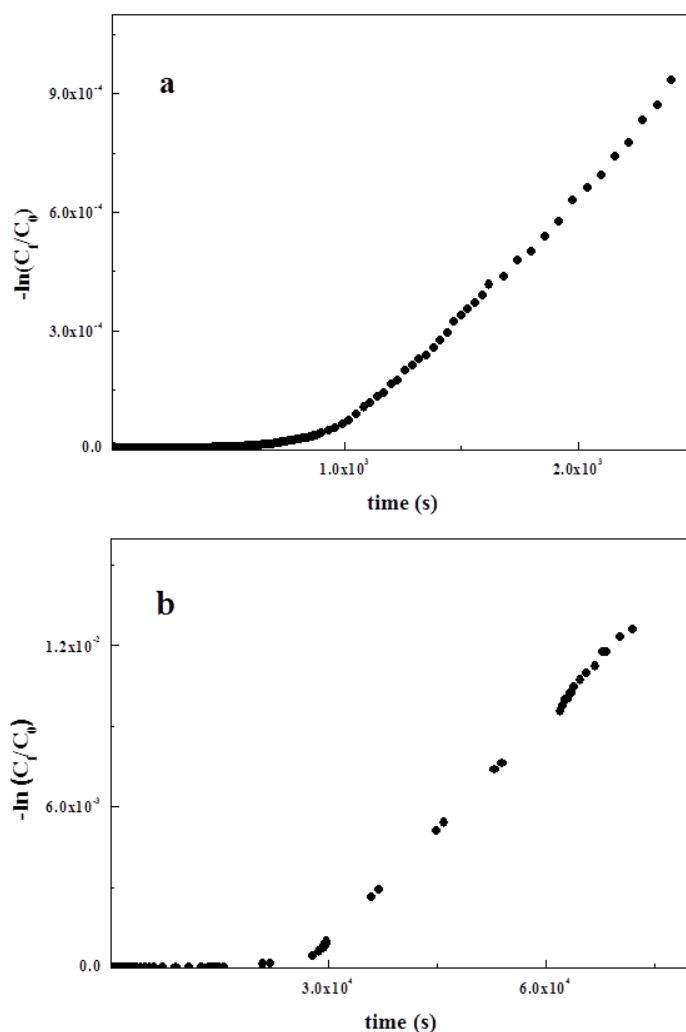


**Figure 6.** Plot of  $-\ln(C_t/C_0)$  versus time for Nafion® N117 (a) and for polymer LPG8 (b) during a proton transport test.

In both cases, the plot exhibits two different regions: the first one, which was much shorter for Nafion® N117 (Figure 6a), corresponds to proton absorption and diffusion across the membrane; once the membranes were saturated by protons, the mechanism became hopping-dominated. One has to keep into account that LPG8 membrane is thicker, with respect to Nafion® N117 membrane; moreover, proton

transport through LPG8 membrane determines some changes in polymer conformation and an increase in its orientation, as it will be shown hereinafter: this could justify the longer time needed for proton diffusion across the membrane. From the slope of the second region, which was quite similar for both materials, we calculated proton permeability.

LPG8 corresponds to a low modification degree (11%) which, in turn, represents high hydroxyl group content and, consequently, is expected to be one of the most hydrophilic copolymers in the series. Therefore, in order to test whether in this case such a remarkable proton transport could be due to the presence of water, in analogy to Nafion<sup>®</sup>, a swelling test was performed. Surprisingly, water uptake resulted as low as 3.1 %. This suggests that water is not crucial for proton transport which occurs instead due to the presence of oriented channels in the membrane. Therefore, alike to modified PECH, these polyglycidol derivatives could be also suitable candidates for the preparation of proton transporting membranes.

In the case of LPG8, it is noteworthy that the XRD pattern of the membrane after transport experiment showed higher degree of order when compared to the fresh oriented membrane. In fact, for the azimuthal scan of the peak at  $2\theta = 2.1^\circ$ , we could observe a decrease of calculated FWHM (Full Width at Half Maximum) from  $186 \pm 6^\circ$  to  $67.2 \pm 0.9^\circ$ . In fact, before transport experiments (Figure S7), the columns are only slightly homeotropically oriented, while, after transport experiments (Figure S8), the peak corresponding to the homeotropically oriented columns is sharper (although some perpendicularly oriented columns can also be evidenced). Thus, transport is able to induce a change in the degree of order of LPG8; this could be favoured by higher chain mobility of this copolymer, which exhibits the lowest modification degree with respect to the other copolymers of the series.

#### 4. Conclusions

We prepared linear polyglycidol with a polymerization degree equal to 20, and subsequently modified it with the dendron 3,4,5-tris[4-(n-dodecan-1-yloxy)benzyloxy]benzoic acid by Steglich esterification with *N,N'*-dicyclohexylcarbodiimide. In this way, we prepared a family of self-assembling LC copolyethers whose modification degrees ranged between 8 and 43%, depending on the –OH/RCOOH molar ratio. On the other hand, the modification degree could not be further improved on increasing reaction time and temperature. The whole copolymer family exhibited LC behavior and the higher the modification degree, the higher the clearing range. It was found that mesophase self-assembling depended on the amount of dendrons introduced: in the case of the lowest modification degree (8%), the copolymer exhibited lamellar columnar packing; in the case of intermediate degrees, the mesophase turned into rectangular columnar while, for the highest modification degrees, hexagonal columnar mesophase was observed. Due to the columnar organization of the copolymers, the polyether backbone is expected to assume a helical conformation, suitable for cation transport through the channel mechanism. Polymer membranes were prepared by immersion precipitation on a fluorinated ethylene propylene (FEP) support. By means of the baking process, we obtained an effective homeotropic orientation of the polymeric columns in the membranes, as confirmed by XRD analysis. Oriented membranes were found to be hydrophobic on both sides of the membrane as shown by their contact angles. The presence of oriented ion channels in the polymeric membranes resulted in remarkable proton permeability, similar to Nafion<sup>®</sup>. Besides, the studied membranes exhibited negligible water uptake after soaking in milli-Q water at room

temperature for 24 hours; therefore, in this case membrane hydration does not seem critical for ion transport.

### ACKNOWLEDGEMENTS

Financial support from CTQ2013-46825-R (Ministerio de Economía y Competitividad) is gratefully acknowledged. The authors are also grateful to Dr. Francesc Guirado for help with the XRD experiments.

### REFERENCES

1. Mauritz KA and Moore RB. *Chem. Rev.* 2004;104:4535-4585
2. Wilhelm FG, Pünt IGM, van der Vegt NFA, Strathmann H, and Wessling M. *Journal of Membrane Science* 2002;199(1–2):167-176.
3. Miyatake K, Chikashige Y, Higuchi E, and Watanabe M. *Journal of the American Chemical Society* 2007;129(13):3879-3887.
4. Li Y, Jin R, Wang Z, Cui Z, Xing W, and Gao L. *Journal of Polymer Science Part A: Polymer Chemistry* 2007;45(2):222-231.
5. Alberti G, Costantino U, Casciola M, Ferroni S, Massinelli L, and Staiti P. *Solid State Ionics* 2001;145(1–4):249-255.
6. Percec V, Johansson G, Heck J, Ungarb G, and Battyb SV. *Journal of the Chemical Society, Perkin Transactions 1* 1993;0(13):1411-1420.
7. Beginn U, Zipp G, and Möller M. *Adv. Mater.* 2000;12:510-513.
8. Yoshio M, Kagata T, Hoshino K, Mukai T, Ohno H, and Kato. *J. Am. Chem. Soc.* 2006;128:5570-5577.

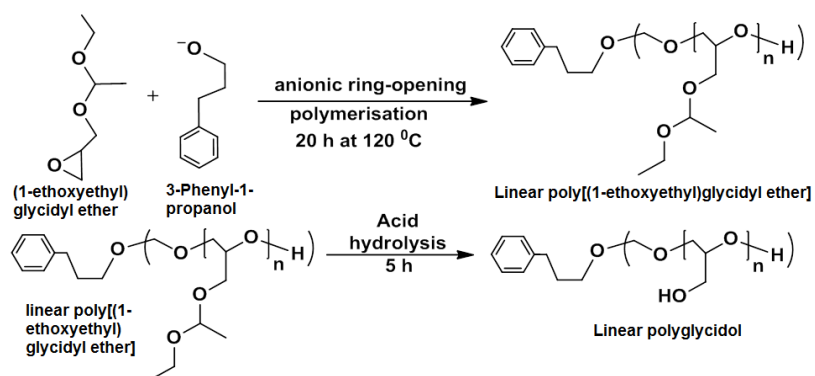
9. Jiménez-García L, Kaltbeitzel A, Pisula W, Gutmann JS, Klapper M, and Müllen K. *Angew. Chem. Int. Ed.* 2009;48:9951-9953.
10. Percec V, Ahn CH, Ungar G, Yeardley DJP, Moller M, and Sheiko SS. *Nature* 1998;391(6663):161-164.
11. Percec V, Glodde M, Bera TK, Miura Y, Shiyarovskaya I, Singer KD, Balagurusamy VSK, Heiney PA, Schnell I, Rapp A, Spiess HW, Hudson SD, and Duan H. *Nature* 2002;417(6905):384-387.
12. Percec V, Schlueter D, Ungar G, Cheng SZD, and Zhang A. *Macromolecules* 1998;31(6):1745-1762.
13. Percec V, Cho W-D, Ungar G, and Yeardley DJP. *Journal of the American Chemical Society* 2001;123(7):1302-1315.
14. Percec V, Imam MR, Peterca M, and Leowanawat P. *J. Am. Chem. Soc.* 2012;134(9):4408-4420.
15. Shi Z, Chen D, Lu H, Wu B, Ma J, Cheng R, Fang J, and Chen X. *Soft Matter* 2012;8:6174-6184.
16. Chuang W-T, Lo T-Y, Huang Y-C, Su C-J, and Jeng U-S. *Macromolecules* 2014;47:6047-6054.
17. Yi Z, Liu X, Jiao Q, Chen E, Chen Y, and Xi F. *J. Polym. Sci.- Part A: Polym. Chem.* 2008;46:4205-4217.
18. Komura M, Yoshitake A, Komiyama H, and Iyoda T. *Macromolecules* 2015;48(3):672-678.
19. Ronda JC, Reina JA, Cádiz V, Giamberini M, and Nicolais L. *Journal of Polymer Science Part A: Polymer Chemistry* 2003;41(19):2918-2929.
20. Ronda JC, Reina JA, and Giamberini M. *Journal of Polymer Science Part A: Polymer Chemistry* 2004;42(2):326-340.

21. Bhosale SV, A.Rasool M, Reina JA, and Giamberini M. *Polymer Engineering and Science* 2013;53(1):159-167.
22. Dulyea LM, Fyles TM, and Robertson GD. *J. Membr. Sci.* 1987;34:87-108.
23. Tylkowski B, Castelao N, Giamberini M, Garcia-Valls R, Reina JA, and Gumí T. *Materials Science and Engineering C* 2012;32(2):105-111.
24. Šakalytė A, Reina JA, and Giamberini M. *Polymer* 2013;54(19):5133-5140.
25. Schmitz C, Keul H, and Möller M. *European Polymer Journal* 2009;45(9):2529-2539.
26. Otera J and Nishikido J. *Esterification: Methods, Reactions, and Applications*: John Wiley & Sons, 2010.
27. Mulder M. *Basic principles of membrane technology*, 2nd ed. The Netherlands: Kluwer Academic Publishers, 2003.
28. Fitton AO, Hill J, Jane DE, and Millar R. *Synthesis* 1987;1987(12):1140-1142.
29. Neises B and Steglich W. *Angewandte Chemie International Edition in English* 1978;17(7):522-524.
30. Hassner A and Alexanian V. *Tetrahedron Letters* 1978;19(46):4475-4478.
31. Goodman LM, Toniolo C, and Felix A. *Houben-Weyl Methods in Organic Chemistry*, 4th ed.: Thieme Publishers, 2003.

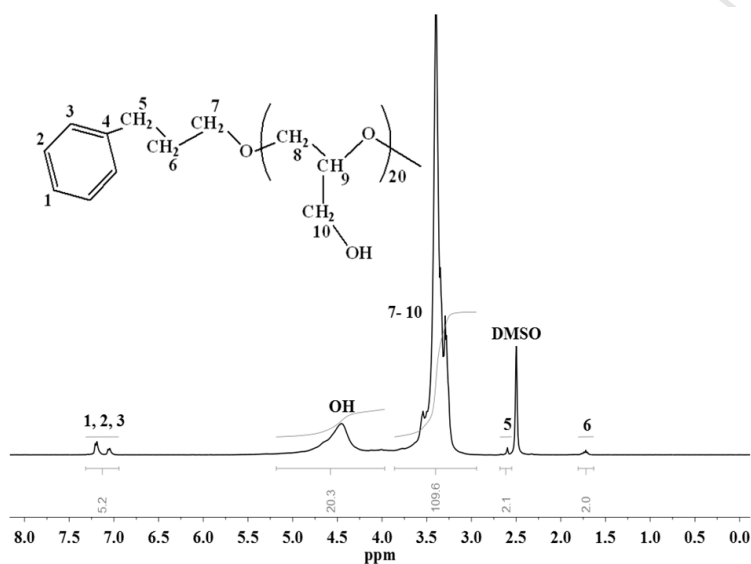
**Highlights**

- Linear polyglycidol was synthesized and modified at different extent with dendritic groups
- Obtained copolymers showed different mesophases, depending on the modification degree
- Oriented membranes could be successfully prepared out of these copolymers
- Oriented membranes showed promising proton permeability and negligible water uptake

## Supplementary information



Scheme S1. Synthesis of linear polyglycidol

Figure S1.  $^1\text{H}$  NMR spectrum of linear polyglycidol in  $^d\text{DMSO}$

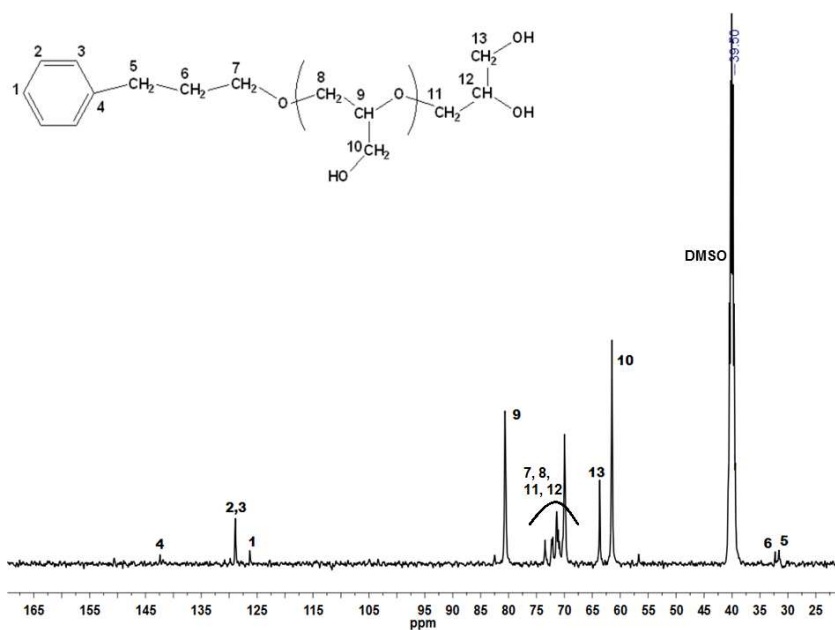


Figure S2.  $^{13}\text{C}$  NMR spectrum of linear polyglycidol in  $^d\text{DMSO}$

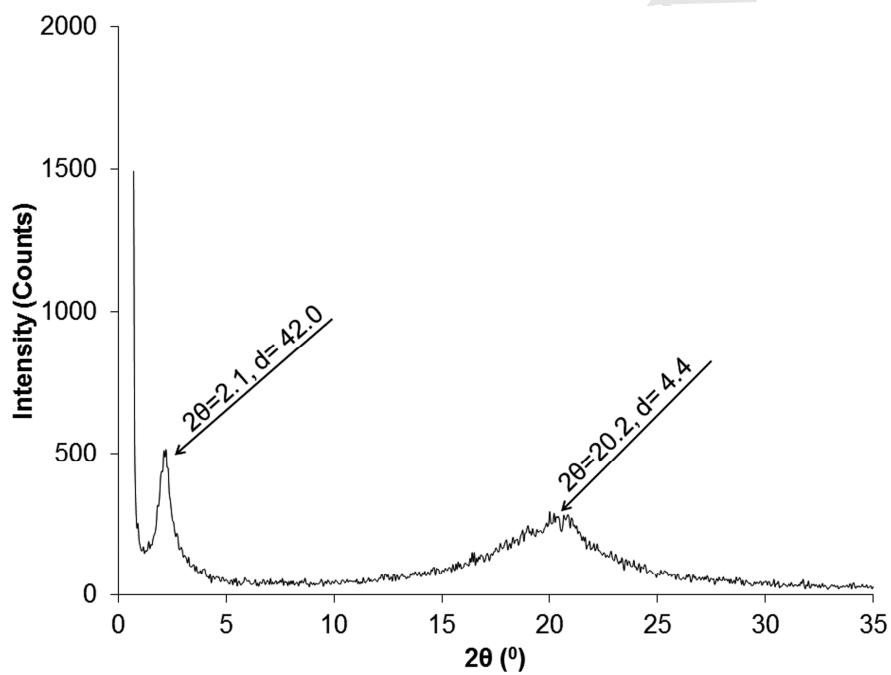


Figure S3. XRD pattern of LPG1 at room temperature.

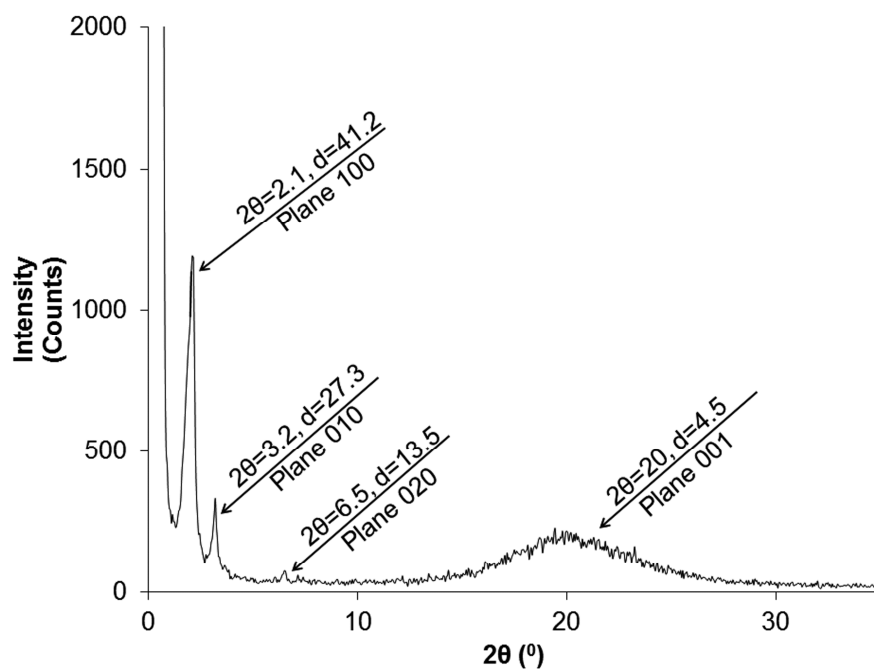


Figure S4. XRD pattern of LPG2 at room temperature.

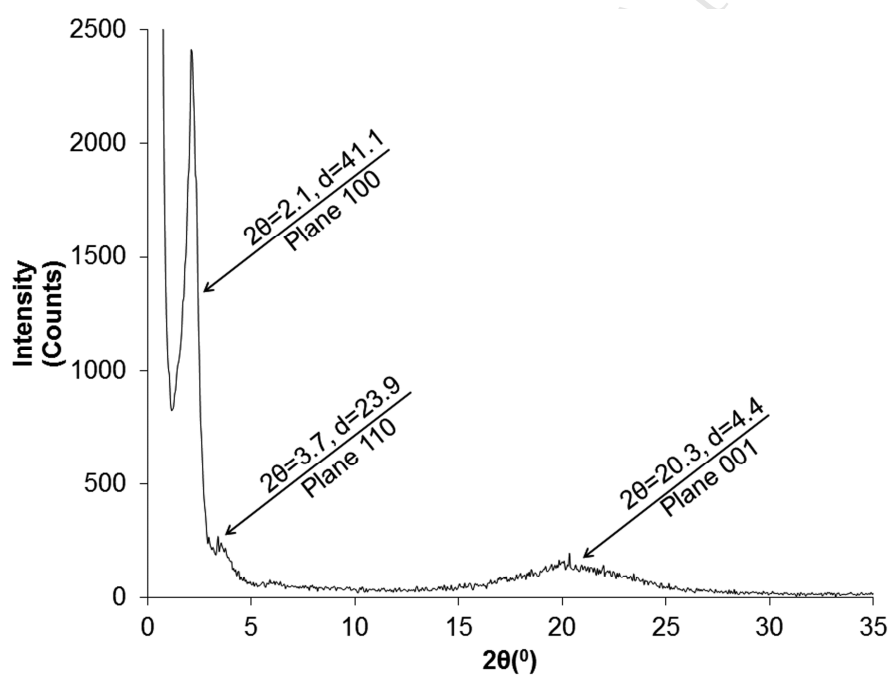
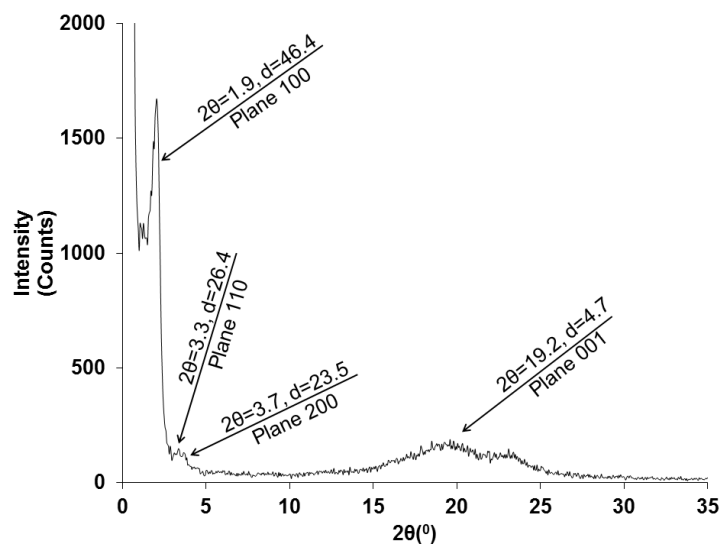
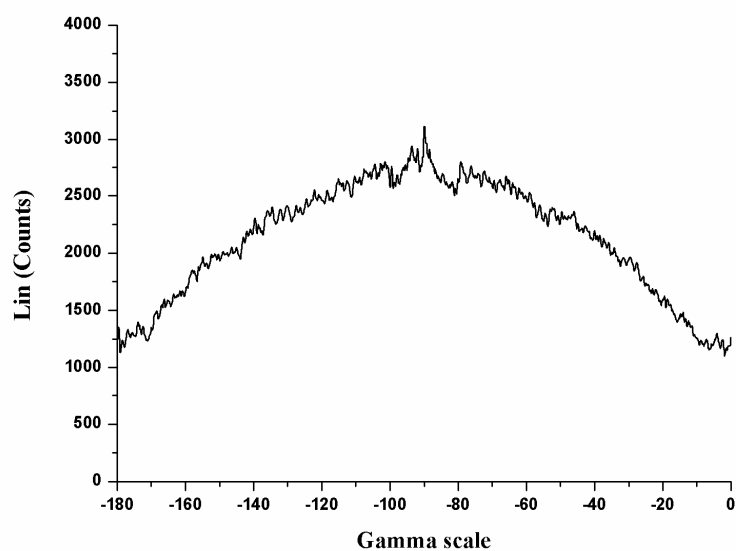


Figure S5. XRD pattern of LPG3 at room temperature.



**Figure S6.** XRD pattern of LPG4 at room temperature.



**Figure S7.** XRD azimuthal intensity plot of LPG8 membrane before permeability test at room temperature ( $2\theta = 2.097^\circ$ ).

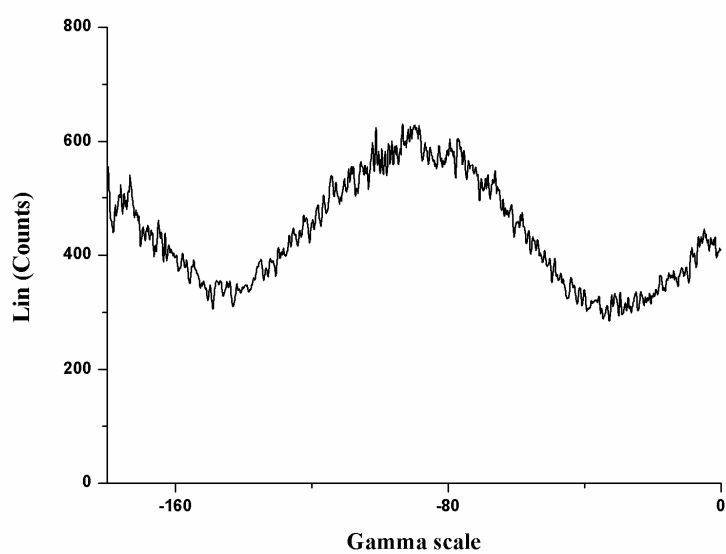


**Figure S8.** XRD azimuthal intensity plot of LPG8 membrane after permeability test at room temperature ( $2\theta = 2.211^\circ$ ).